THERMAL RADIATION PROPERTIES OF TURBULENT LEAN PREMIXED METHANE AIR FLAMES

JUN JI, Y. R. SIVATHANU AND J. P. GORE

M. J. Zucrow Laboratories
School of Mechanical Engineering
Purdue University
West Lafayette, IN 47907-1003, USA

Thermal radiation properties of turbulent premixed flames have received little attention in the past perhaps because of the lower radiative heat loss compared with that for non-premixed flames. However, the high-temperature sensitivity of NO kinetics and the importance of radiation in near-limit laminar premixed flames provide fundamental reasons for studies of radiation properties of turbulent premixed flames. Reduced cooling airflows in lean premixed combustors, miniaturization of combustors, and the possible use of radiation sensors in combustion control schemes are some of the practical reasons for studying radiation heat transfer in these flames. Motivated by this, we report the first (to our knowledge) study of spectral radiation properties of turbulent premixed flames. Measurements of mean, root mean square (rms) and probability density functions (PDFs) of spectral radiation intensities leaving diametric paths at five heights in two turbulent lean premixed methane/air jet flames stabilized using small H_2/air pilot flames in a coflow of air were completed. Measurements of spectral radiation intensities leaving three laminar flames were also completed. These data were used to evaluate narrowband radiation calculations independent of the treatment of turbulent fluctuations. Stochastic spatial series analysis was used to estimate instantaneous distributions of temperature. The analysis requires the specification of mean and rms temperature distributions, integral length scale distributions, and an assumption of exponential spatial correlation function. We specified the mean and rms temperature distributions measured by calibrated narrowband thin filament pyrometry. A simple flame and mixing model was used to relate the concentrations of CO_2 and H_2O to the temperature. We used scalar spatial series in conjunction with a radiation model to calculate the mean, rms, and PDFs of spectral radiation intensities. Overall, the model predictions are in reasonable agreement with the data. The only improvement needed is in the area of capturing correlated occurrences of high temperatures along the radiation path.

Introduction

Radiation properties of non-premixed turbulent flames have been widely studied both experimentally and theoretically [1–6]. Non-premixed flames radiate between 10% and 60% of their chemical energy release depending on fuel type. The radiation predominantly involves emission from soot, CO_2, and H_2O [1]. The effects of turbulence on radiation in non-premixed flames have been well documented [1–6].

Radiation properties of turbulent premixed flames have not received much attention except for early computations in Ref. [7], where the effects of turbulence on radiation properties of a two-dimensional premixed methane/air flame in a furnace were analyzed. However, experimental data were not available for model validation. The lack of attention to turbulent premixed flame radiation in the past could be because of the relatively small radiative heat loss, at least for atmospheric pressure conditions.

Effects of radiation heat loss on the lean flammability limit and on the propagation speeds of near-limit laminar premixed flames have been long recognized (see Refs. [8,9] and their citations). These papers contain interesting findings regarding radiation-induced bifurcations [8] and effects of self-absorption of radiation [9]. Premixed flames are more prone to instability and their radiation signals may be used in a control strategy. Motivated by this, the present work is devoted to measurements and time and space series analysis of spectral radiation properties of turbulent premixed flames.

The effects of turbulent fluctuations on radiation result from the nonlinear dependence of the Planck function and the absorption coefficient on species concentrations and temperature. The control strategy discussed above must account for the radiation fluctuations.

The present work consisted of the following:

1. Mean, root mean square (rms), and probability density function (PDF) of the spectral radiation

Report Documentation Page	Form Approved OMB No. 0704-0188

Public reporting burden for the collection of information is estimated to average 1 hour per response, including the time for reviewing instructions, searching existing data sources, gathering and maintaining the data needed, and completing and reviewing the collection of information. Send comments regarding this burden estimate or any other aspect of this collection of information, including suggestions for reducing this burden, to Washington Headquarters Services, Directorate for Information Operations and Reports, 1215 Jefferson Davis Highway, Suite 1204, Arlington VA 22202-4302. Respondents should be aware that notwithstanding any other provision of law, no person shall be subject to a penalty for failing to comply with a collection of information if it does not display a currently valid OMB control number.

1. REPORT DATE **04 AUG 2000**	2. REPORT TYPE **N/A**	3. DATES COVERED **-**

4. TITLE AND SUBTITLE **Thermal Radiation Properties of Turbulent Lean Premixed Methane Air Flames**	5a. CONTRACT NUMBER
	5b. GRANT NUMBER
	5c. PROGRAM ELEMENT NUMBER
6. AUTHOR(S)	5d. PROJECT NUMBER
	5e. TASK NUMBER
	5f. WORK UNIT NUMBER

7. PERFORMING ORGANIZATION NAME(S) AND ADDRESS(ES) **School of Mechanical Engineering Purdue University West Lafayette, IN 47907-1003, USA**	8. PERFORMING ORGANIZATION REPORT NUMBER

9. SPONSORING/MONITORING AGENCY NAME(S) AND ADDRESS(ES)	10. SPONSOR/MONITOR'S ACRONYM(S)
	11. SPONSOR/MONITOR'S REPORT NUMBER(S)

12. DISTRIBUTION/AVAILABILITY STATEMENT
Approved for public release, distribution unlimited

13. SUPPLEMENTARY NOTES
See also ADM001790, Proceedings of the Combustion Institute, Volume 28. Held in Edinburgh, Scotland on 30 July-4 August 2000. , The original document contains color images.

14. ABSTRACT

15. SUBJECT TERMS

16. SECURITY CLASSIFICATION OF:			17. LIMITATION OF ABSTRACT	18. NUMBER OF PAGES	19a. NAME OF RESPONSIBLE PERSON
a. REPORT **unclassified**	b. ABSTRACT **unclassified**	c. THIS PAGE **unclassified**	**UU**	**8**	

intensities leaving diametric paths in a turbulent lean premixed methane/air jet flame were measured.

2. The temperature statistics in the flame were measured using narrowband thin filament pyrometry (TFP) calibrated using measurements in laminar flat flames.

3. A stochastic time and space series analysis was constructed following Ref. [3] to predict the flame radiation statistics. The temperature measurements and a combustion/mixing model were utilized to estimate the species concentration time series in conjunction with local, mean equivalence ratio measurements. The radiation model was independently verified using measurements in two additional laminar flames.

Background

Axisymmetric Premixed Turbulent Flames

Axisymmetric pilot-stabilized Bunsen-type turbulent premixed flames identical to those previously used in this laboratory [10] were considered. Many others [11–18] have used this flame configuration. Many of these studies involved temperature and velocity measurements [11–14,16]. Some studies have involved visualization of flame surfaces and integral length scales of wrinkling [15]. To our knowledge, work has not been reported on the radiation characteristics of axisymmetric turbulent premixed jet flames.

Thin Filament Pyrometry

Accurate measurements of temperature time series are essential for evaluation of turbulent radiation properties. Pitts [19] has shown that TFP, originally introduced by Vilimpoc and Goss [20], has the potential to provide 5 to 10 K precision and accuracy for flame temperature measurements. This technique can provide a 1 ms time response with $120\,\mu m$ resolution and a high signal-to-noise ratio above 1000 K.

Temperature profiles in diffusion flames, partially premixed flames, and turbulent premixed flames have been measured using broadband TFP [21–23]. With a liquid nitrogen cooled InSb detector operating over a range of wavelengths between 1.1 μm and 5.7 μm, temperatures as low as 500 K could be measured. Broadband TFP often suffers from a strong flame emission signal. Such a signal can be properly subtracted for laminar flames [21,22]. However, for turbulent flames, accurate correction is impossible.

Motivated by this, Bedat et al. [24] developed a narrowband TFP technique, which utilizes a spectral window centered at 3.9 μm to avoid flame emission

from gaseous molecules. With liquid nitrogen cooled InSb, they could also measure temperatures as low as 500 K. A heated tungsten filament combined with a blackbody was used for calibration. This approach is adequate for non-sooty flames. Therefore, the present measurements utilized a similar approach with the narrowband filter of Ref. [24] replaced with a monochromator. In addition, calibration of the system was performed using a flat laminar premixed flame and emission spectroscopy as the primary standard.

Experimental Methods

Laminar Flat Flames

The laminar, premixed flat flames were established on a McKenna burner. The premixed methane/air gases flowed out from the central port, which had a diameter of 60 mm. An annular coflow of air (0.9 g/s) with an outer diameter of 75 mm was included. A constant airflow rate of 0.36 g/s was used for the central port. Flames with three equivalence ratios (ϕ = 0.6, 0.54, and 0.46) were established by varying the fuel mass flow rate. Choked orifice meters controlled all flow rates. The equivalence ratio settings also were checked with sampling and gas chromatography. The operating conditions were selected to avoid cellular instabilities while providing near-adiabatic conditions. Thermocouple (Pt, Pt-Rh10% with 0.3 mm bead diameter) traverses were utilized to ensure flat temperature profiles and to measure the length of the homogeneous radiating path.

Turbulent Premixed Flames

The turbulent flame burner and operating conditions were identical to those used in Refs. [10] and [25,26]. Premixed methane/air flowed through a 15 mm diameter inner cylindrical tube surrounded by a 102 mm diameter outer airflow casing. The length of the central tube ensured a fully developed turbulent pipe flow. A pilot flame burner consisting of 90 fine ports with a diameter of 0.2 mm uniformly distributed along a mean diameter of 20 mm was mounted at the exit. A hydrogen (2 mg/s) diffusion pilot flame was used. The operating conditions involved equivalence ratios of 0.8 and 1 for flames burning with a heat release rate of 4.2 kW. The fuel flow rate was 84 mg/s and the airflow rates were 2000 and 1340 mg/s. The coflow airflow rate was maintained at 540 mg/s. The effects of the hydrogen pilot were observed only within the first 5 mm. The ϕ = 1, 0.8 flames had burner exit Reynolds numbers of 7000 and 8700, respectively.

Species Concentration Measurements

Measurements of species concentrations were obtained using sampling and gas chromatography (Shimadzu GC14A). The samples were obtained using a

quartz microprobe with an outer diameter of 0.5 mm and an inner diameter of 80 μm using an evacuated bulb method [27]. The samples were dried, separated using Chromosorb 102 and molecular sieve 5A columns, and analyzed using a calibrated detector. The dry-based measurements were used to calculate the equivalence ratio using a constant C/H ratio and a correction for argon to the apparent O_2 measurement. The uncertainties in the measured equivalence ratios were less than 10%.

Measurements of Spectral Radiation Intensities

The spectral radiation leaving diametric paths at a fixed height above the laminar and the turbulent flame burners was collimated by a 308 mm long, 4 mm diameter tube coated with black paint. A 1/8 m monochromator (Oriel model 77250) with adjustable slits and a liquid N_2 cooled InSb detector (Graseby Infrared model U-1933-S) were used. The output of the detector was amplified and conditioned by a preamplifier (Graseby Infrared model U-3237). An optical chopper (Model SR540 Stanford Research Systems, Inc.) was set at 3000 Hz for the turbulent flame measurements. The output of the preamplifier was fed to a Lock-In amplifier (Stanford Research Inc. model SR510). The Lock-In amplifier was modified to allow frequency response up to 5000 Hz. The output signal was sent to a laboratory computer via an A/D board, CIO-DAS16/M1 (Computer Board, Inc). A high pass optical filter set at 2.5 μm was used. The slits were set to obtain a bandwidth of $\Delta\lambda = 12$ nm. The frequency settings for the laminar flame measurements were a factor of 100 lower than those summarized above.

A grating (Oriel Model 77301) operational over the wavelength range of 2.5–8 μm was used to cover the spectral range of interest for the CO_2 and H_2O band emission in the mid-infrared for the lean premixed flames. In the current arrangement, the accuracy and the precision of the wavelength adjustment were 8 nm and 1.6 nm, respectively.

A blackbody (Infrared Industries, Model IR-563) operated at three different temperatures (1100, 1200, and 1300 K) was used to calibrate the system, and the linearity of the calibration was within 1%. Experimental uncertainties (95% confidence level) for the laminar and turbulent flame measurements were less than 2% and 5%, respectively. The measurements were repeatable within these limits.

Narrowband Thin Filament Pyrometry

A single SiC fiber with a diameter between 10 and 20 μm was stretched across a holder with 100 mm spacing between two lubricated pulleys. Small weights attached at each end of the fiber kept it taut in the flame. The present narrowband TFP utilized the entire spectral radiation intensity measurement apparatus discussed above, except for the collimating tube. Instead, two 100 mm diameter CaF_2 lenses were used to focus the emission signal from approximately 250 μm length of the SiC fiber onto the InSb detector. The monochromator was set at a wavelength of $\lambda = 3.82$ μm to avoid flame emission, with a bandwidth $\Delta\lambda = 0.15$ μm to allow adequate signal.

The narrowband TFP has excellent precision (5 K). Proper calibration of the fiber and the associated optics and electronics is needed for obtaining good accuracy. Unfortunately, different researchers have followed different calibration techniques. In the present work, emission spectroscopy for one laminar flame was used as the primary calibration method in conjunction with a radiation model. The TFP measurements were then checked against the adiabatic flame temperatures, which were calculated using measured species concentrations. The net result was that an estimated accuracy of 30 K was achieved with the present procedure at a measurement temperature of 1500 K (1.5%).

The radiation corrections to the TFP data in the laminar flames were calibrated out because of the constant convection velocity over the fiber for the different operating conditions. For the turbulent flames, an energy balance over the fiber involving heat transfer from the hot gas and radiation to the black cold surroundings was performed. An empirical correlation between the Nusselt and the Reynolds number was used [28]. The Nusselt number was evaluated using the measured mean velocity and the fiber diameter as the quantities needed for defining the Reynolds number. Based on the magnitude of the radiation correction, the uncertainties in the correction introduced approximately 30 K additional inaccuracies in the estimated gas temperatures.

Theoretical Methods

We avoided the uncertainties of the flame structure models in the radiation predictions by utilizing the measured mean and rms temperatures to generate time and space series in the present calculations. The combined reaction progress variable and mixture fraction approach of Ref. [10] was utilized.

The instantaneous temperature is a function of the reaction progress variable and the local mixture fraction. The mixture fraction is equal to unity for the material (fuel and air) flowing from the burner tube and zero for the coflow air. The reaction proceeds to completion prior to mixing of the coflow air [10]. This was applied on an instantaneous basis here. Thus, if the equivalence ratio was equal to that of the incoming mixture, the temperature and species mass fractions were uniquely related to the respective reaction progress variables. The progress variables based on temperature and product species concentrations were assumed to be identical.

$$c = \frac{T_p - T}{T_p - T_r} = \frac{Y_{CO_2}}{Y_{CO_2P}} = \frac{Y_{H_2O}}{Y_{H_2OP}} \qquad (1)$$

where c is the reaction progress variable calculated using the temperature T, and Y_{CO_2} and Y_{H_2O} are calculated using the c and the values of these quantities in the product stream (denoted by subscript P). T_p is the peak-measured temperature, and T_r is the incoming fuel/air mixture temperature. This assumption was not valid in the flame zone and for non-unity Lewis numbers because of the multiple steps involved in the detailed chemistry process. The facts that the reaction zones were relatively thin and that the Lewis numbers were close to unity for the mixtures under consideration may control the errors caused by the simplification.

If the measured mean equivalence ratio was less than that of the incoming mixture, then the species concentrations were calculated as

$$Z = \frac{T_p - T}{T_p - T_c} = \frac{Y_{CO_2}}{Y_{CO_2P}} = \frac{Y_{H_2O}}{Y_{H_2OP}} \qquad (2)$$

where T_c is the temperature of the coflow air and Z is the mixture fraction defined as the mass of the incoming mixture divided by the total mass at a location beyond the flame sheet. Use of detailed chemistry calculations had little effect on the present conclusions.

Once the species concentrations time series are determined from the temperature time series, the radiation calculations can be performed if these quantities are known at all points along the radiation path. The time and space series analysis described the instantaneous temperature fluctuation at a point $s + \Delta s$ along the radiation path at time $t + \Delta t$ as

$$\frac{T'(s + \Delta s, t + \Delta t)}{(\overline{T'(s + \Delta s)^2})^{1/2}} = \phi_1 \frac{T'(s, t + \Delta t)}{(\overline{T'(s)^2})^{1/2}}$$
$$+ \phi_2 \frac{T'(s + \Delta s, t)}{(\overline{T'(s + \Delta s)^2})^{1/2}} + a(s + \Delta s, t + \Delta t) \qquad (3)$$

The first two terms on the right-hand side represent the correlated fluctuation in temperature, where ϕ_1 and ϕ_2 are related to the temporal and spatial correlation coefficients as

$$\phi_1 = \frac{\rho(\Delta s) - \rho(\Delta t)\rho(\Delta s, \Delta t)}{1 - \rho^2(\Delta s, \Delta t)}$$

$$\phi_2 = \frac{\rho(\Delta t) - \rho(\Delta s)\rho(\Delta s, \Delta t)}{1 - \rho^2(\Delta s, \Delta t)} \qquad (4)$$

The third term $a(s + \Delta s, t + \Delta t)$ is the random part of the temperature fluctuation whose mean value is zero and the mean square value is given as

$$\overline{a^2}(s + \Delta s, t + \Delta t) = 1 - \phi_1^2$$
$$- \phi_2^2 - 2\phi_1\phi_2\rho(\Delta s, \Delta t) \qquad (5)$$

where the correlation coefficients are given as

$$\rho(\Delta s) = \frac{\overline{T'(s + \Delta s, t + \Delta t)T'(s, t + \Delta t)}}{(\overline{T'(s + \Delta s)^2})^{1/2}(\overline{T'(s)^2})^{1/2}}$$

$$\rho(\Delta t) = \frac{\overline{T'(s + \Delta s, t + \Delta t)T'(s + \Delta s, t)}}{\overline{T'(s + \Delta s)^2}} \qquad (6)$$

$$\rho(\Delta s, \Delta t) = \frac{\overline{T'(s + \Delta s, t)T'(s, t + \Delta t)}}{(\overline{T'(s + \Delta s)^2})^{1/2}(\overline{T'(s)^2})^{1/2}}$$

In the present simulations the correlation coefficients were modeled as

$$\rho(\Delta s) = \exp\left(-\frac{\Delta s}{l_1}\right), \rho(\Delta t) = \exp\left(-\frac{\Delta t}{\tau_1}\right),$$
$$\rho(\Delta s, \Delta t) = \rho(\Delta s)\rho(\Delta t) \qquad (7)$$

where l_1 is integral length scale of turbulent temperature fluctuations and τ_1 is the integral time scale of turbulent temperature fluctuations. There is some support for the exponential nature of the spatial and temporal correlation coefficients from non-reacting jet and non-premixed flame literature. However, the present extension to premixed flame radiation is a first step, justified only by the lack of relevant information.

Spectral radiation intensities were found by solving the equation of radiative transfer covering 2.5 to 5 μm wavelength range. This range covers the two important bands of CO_2 and one important band of H_2O. Narrowband analyses in RADCAL [29] were utilized. A more recent model [30] was also considered but did not produce any improvements for the present conditions.

For a homogeneous path of known length and known components of the participating medium in the laminar TFP calibration flame, RADCAL is used in an inverse iterative procedure to find the temperature and concentrations from the measurements of spectral radiation intensities. From the calculated CO_2 and H_2O concentrations, the equivalence ratio is also estimated.

Results and Discussion

Laminar Flames

Figure 1 shows the measurements and predictions of spectral radiation intensities for the laminar flat flames. The $\phi = 0.54$ flame was used for TFP cal-
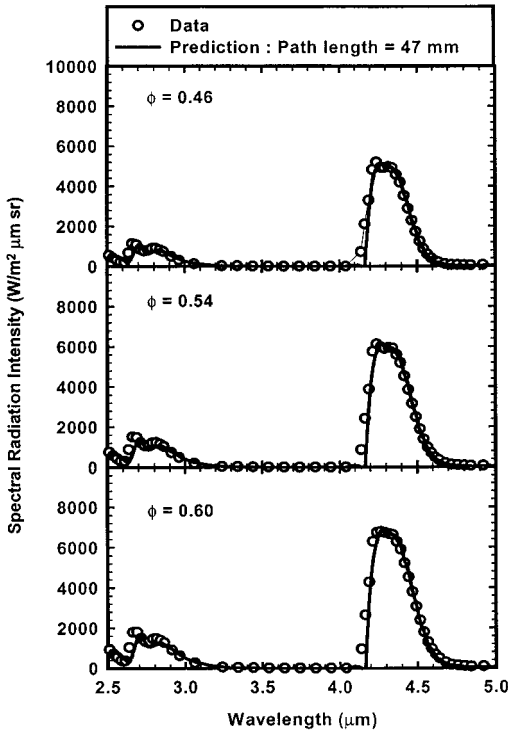
FIG. 1. Measurements and predictions of spectral radiation intensities in laminar premixed flat flames.

TABLE 1
Comparison of measurements and predictions of
temperature and equivalence ratio for laminar flat flames

ϕ_{GC}	0.46	0.54	0.60
ϕ_{ES}	0.48	0.53	0.59
T_{TFP} (K)	1384	1498	1591
T_{ES} (K)	1395	1498	1558
T_{ADB} (K)	1402	1499	1600

ibration. Therefore, the agreement between measurements and predictions for this flame illustrates the efficacy of the inverse procedure. The TFP measured temperatures for the other two flames were used in conjunction with RADCAL to predict the spectral radiation intensities. The agreement (cumulative error of less than 1% over all wavelengths) between the measurements and the predictions for these two flames supports the RADCAL model. A comparison of the equivalence ratios and temperatures is shown in Table 1. The agreement between the emission spectroscopy and TFP data and the adiabatic temperature estimates shows excellent internal consistency.
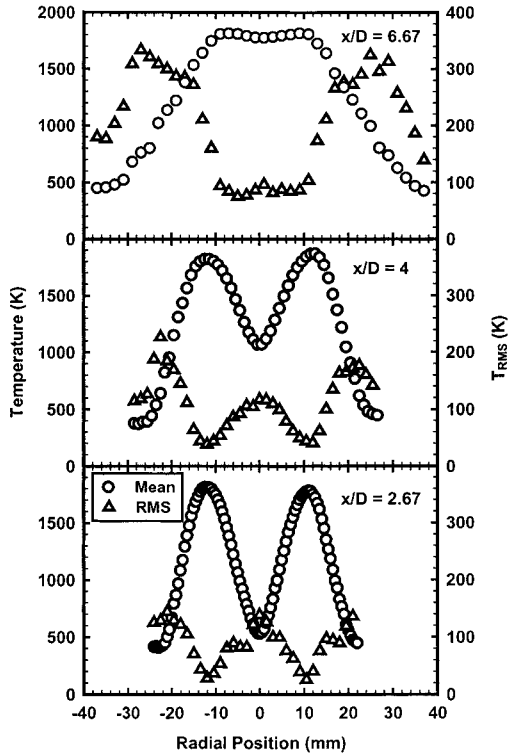

FIG. 2. Measurements of mean and rms temperature distributions at x/D = 2.67, 4, and 6.67 in a ϕ = 0.8, Q = 4.2 kW lean premixed turbulent flame.

Turbulent Flames

Measurements for the Q = 4.2 kW, ϕ = 0.8 flame are considered as an example. Fig. 2 shows the measurements of mean and rms temperatures along diametric paths within the flame at three heights. The peak mean temperatures are close to 1900 K at all three positions. The x/D = 6.67 location is very close to the flame tip. The rms temperatures near the peak temperature locations are very low, but they increase significantly near the edge and near the flame tip.

The measurements of mean equivalence ratio are shown in Fig. 3. The data show that the equivalence ratio remains close to the 0.8 value for a wide region near the axis and then decreases to the value of zero in the coflow. In the present model, these data are used to select either the progress variable based (equation 1) or the mixture fraction based (equation 2) relationship between temperature and species concentrations.

Figure 4 shows measurements and predictions of mean spectral radiation intensity for the turbulent flame at the three locations. The baseline integral
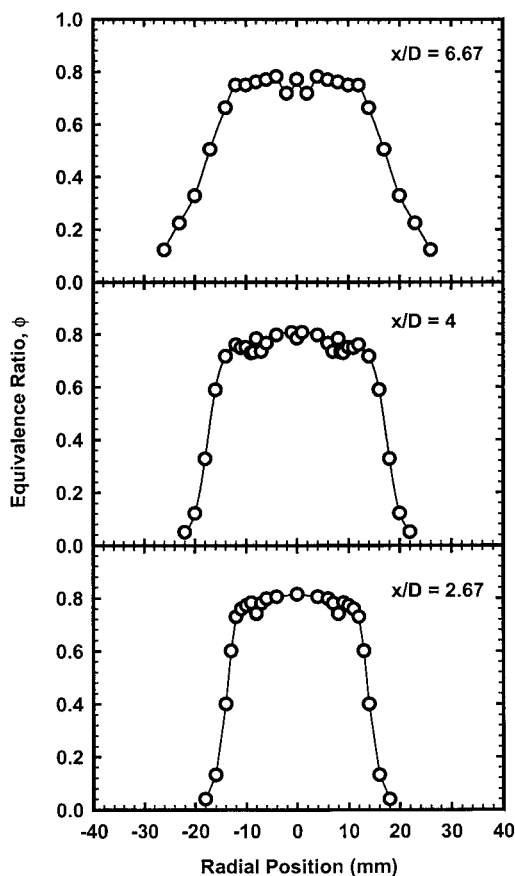
FIG. 3. Measurements of mean equivalence ratio distributions at x/D = 2.67, 4, and 6.67 in a ϕ = 0.8, Q = 4.2 kW lean premixed turbulent flame.

FIG. 4. Measurements and predictions of mean spectral radiation intensity at x/D = 2.67, 4, and 6.67 in a ϕ = 0.8, Q = 4.2 kW lean premixed turbulent flame.

length scale for turbulent fluctuations was selected to be 4 mm based on past estimates [25,26]. The timescale was calculated based on the prescribed length scale and mean velocity data from Ref. [25] in conjunction with Taylor's hypothesis. The predicted mean spectral intensity is independent of the choice of the length scale as shown by the calculations with two additional length scales for the x/D = 2.67 and x/D = 6.67 locations.

Figure 5 shows the rms data and predictions of the spectral radiation intensities. The agreement between the measurements and predictions with the 4 mm integral length scale are excellent for the x/D = 4 position. However, the rms is overpredicted at x/D = 2.67 and underpredicted at x/D = 6.67. If the integral length scale is reduced to 2 mm at x/D = 2.67 and increased to 8.5 mm at x/D = 6.67, excellent agreement between measured and predicted spectra is achieved. The monotonic increase of integral length scale from 2 mm at x/D = 2.67 to
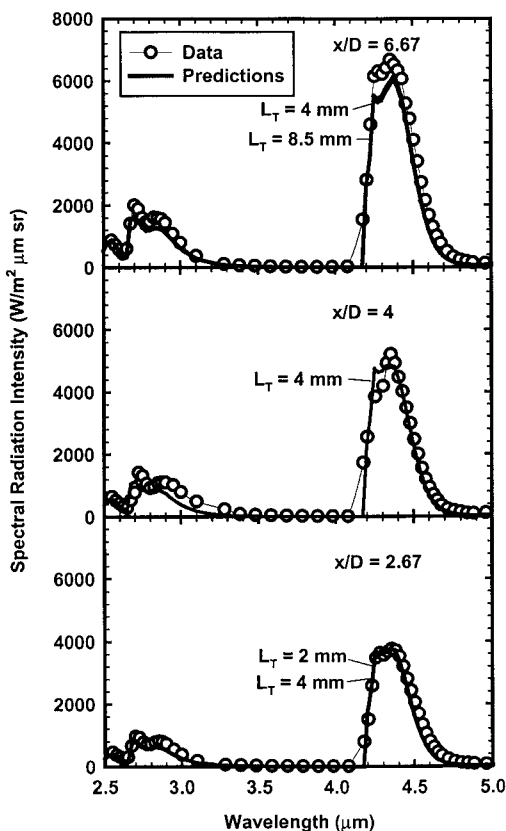
8.5 mm at x/D = 6.67 is qualitatively consistent with similarity scaling. However, integral length scale data are necessary to independently confirm these findings.

Figure 6 shows measurements and predictions of PDFs of spectral radiation intensities. Gaussian curves are included for reference. The analysis misses the highest intensity excursions, suggesting that the correlated occurrence of highest temperatures (flames) is not captured. However, the level of agreement is quite satisfactory considering that this is the first attempt at predicting radiation statistics of turbulent premixed flames.

Conclusions

1. Measurements and predictions of spectral radiation intensities in laminar flames show that the RADCAL algorithm and constants yield excellent results for the present conditions. Based on this, emission spectroscopy can be used as an absolute
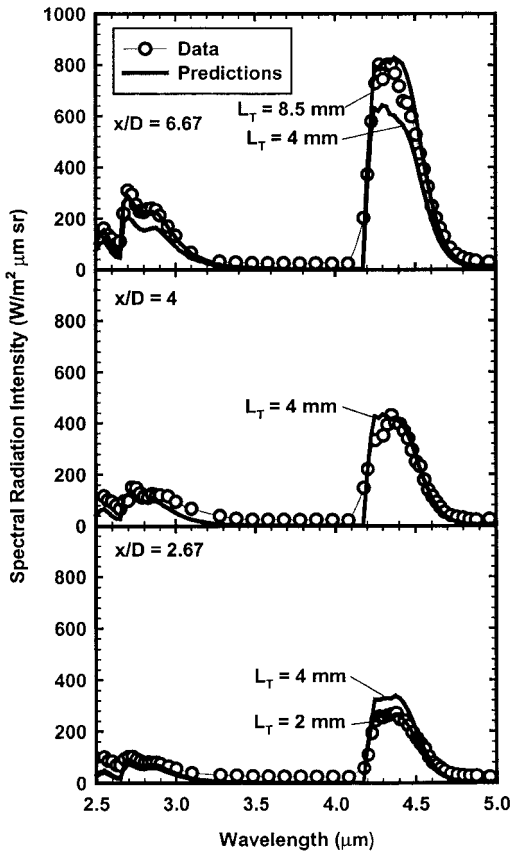
FIG. 5. Measurements and predictions of rms of spectral radiation intensity at $x/D = 2.67$, 4, and 6.67 in a $\phi = 0.8$, $Q = 4.2$ kW lean premixed turbulent flame.
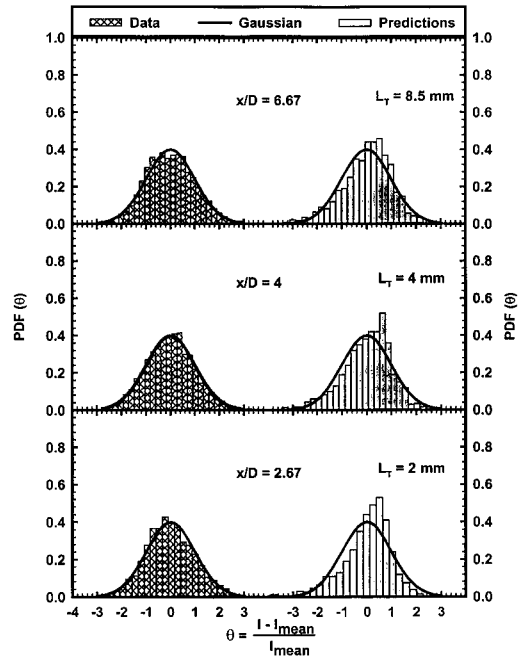

FIG. 6. Measurements and predictions of PDFs of spectral radiation intensities at $x/D = 2.67$, 4, and 6.67 in a $\phi = 0.8$, $Q = 4.2$ kW lean premixed turbulent flame.

standard for calibration of thin filament pyrometry.

2. Measurements of mean equivalence ratio show that a model involving premixed combustion at the burner tube equivalence ratio followed by mixing with the coflow air may be adequate for these flames.

3. Measurements and predictions of mean and rms spectral radiation intensities for the turbulent flame show excellent agreement with each other if the integral length scale of temperature fluctuations is calibrated.

4. The occurrence of correlated highest intensity events is missed by the present analysis based on a comparison of the measured and predicted PDFs of intensity.

Acknowledgment

REFERENCES

1. Faeth, G. M., Gore, J. P., Chuech, S. G., and Jeng, S-M., in *Annual Reviews of Numerical Fluid Mechanics and Heat Transfer* (C. L. Tien and T. C. Chawla, eds.), Hemisphere, New York, 1989, pp. 1–38.

2. Gore, J. P., and Faeth, G. M., *Proc. Combust. Inst.* 21:1521–1531 (1986).

3. Kounalakis, M. E., Gore, J. P., and Faeth, G. M., *Proc. Combust. Inst.* 22:1281–1290 (1988).

4. Hartick, J. W., Tacke, M., Fruchtel, G., Hassel, E. P., and Janicka, J., *Proc. Combust. Inst.* 26:75–82 (1996).

5. Bressloff, N. W., Moss, J. B., and Rubini, P. A., *Proc. Combust. Inst.* 26:2379–2386 (1996).

6. Krebs, W., Koch, R., Ganz, B., Eigenmann, L., and Wittig, S., *Proc. Combust. Inst.* 26:2763–2770 (1996).

7. Song, T. H., and Viskanta, R., *J. Thermophys.* 1(1):56–62 (1987).

8. Ju, Y., Masuya, G., Liu, F., Guo, H., Maruta, K., and Niioka, T., *Proc. Combust. Inst.* 27:2551–2557 (1998).

9. Ju, Y., Masuya, G., and Ronney, P. D., *Proc. Combust. Inst.* 27:2619–2626 (1998).

10. Prasad, R. O. S., Paul, R. N., Sivathanu, Y. R., and Gore, J. P., *Combust. Flame* 117:514–528 (1999).

11. Yoshida, A., and Tsuji, H., *Proc. Combust. Inst.* 17:945–956 (1979).

12. Yoshida, A., *Proc. Combust. Inst.* 18:945–956 (1981).

13. Shepherd, I. G., and Moss, J. B., *AIAA J.* 20:566–569 (1981).

14. Yanagi, T., and Mimura, Y., *Proc. Combust. Inst.* 18:1031–1039 (1981).

15. Chew, T. C., Britter, R. E., and Bray, K. N. C., *Combust. Flame* 80:65–82 (1990).

16. Wu, M. S., Kwon, S., Driscoll, J. F., and Faeth, G. M., *Combust. Sci. Technol.* 73:327–350 (1991).

17. Zhang, Y., and Bray, K. N. C., *Prog. Astronaut. Aeronaut.* 152:56–69 (1993).

18. Chen, Y. C., Peter, N., Schneemann, G. A., Wruck, N., Renz, U., and Mansour, M. S., *Combust. Flame* 107:223–244 (1996).

19. Pitts, W. M., *Proc. Combust. Inst.* 26:1171–1179 (1996).

20. Vilimpoc, V., and Goss, L. P., *Proc. Combust. Inst.* 22:1907–1914 (1998).

21. Blevins, L. G., Renfro, M. W., Laurendeau, N. M., Lyle, K. H., and Gore, J. P., *Combust. Flame* 118:684–696 (1999).

22. Ravikrishna, R. V., and Laurendeau, N. M., in *Proceedings of the Technical Meeting of the Central States Section of the Combustion Institute,* The Combustion Institute, Pittsburgh, PA, 1998, pp. 297–302.

23. Chen, T. H., and Goss, L. P., *J. Prop. Power* 8:16–20 (1992).

24. Bedat, B., Giovannini, A., and Pauzin, S., *Exp. Fluids* 17:397–404 (1994).

25. Kelkar, A. S., "Flowfield Statistics and Pollutant Emission Indices of Piloted Turbulent Lean Premixed Flames," M.S. thesis, Purdue University, West Lafayette, IN, 1996.

26. Chakka, R. K., "An Experimental Investigation of Scalar Properties of Piloted Turbulent Lean Premixed Flames," M.S. thesis, Purdue University, West Lafayette, IN, 1996.

27. Gore, J. P., and Skinner, S. M., *Combust. Flame* 87:357–364 (1991).

28. Morgan, V. T., *Adv. Heat Transfer* 11:199–264 (1975).

29. Grosshandler, W. L., *NIST Technical Note 1402,* NIST, Gaithersburg, MD, 1993.

30. Soufiani, A., and Taine, J., *Int. J. Heat Mass Transfer* 40:987–991 (1997).

COMMENTS

Friedrich Dinkelacker, University of Erlangen, Germany. What is a typical amount of temperature reduction due to radiation, for example, for a laminar or slightly turbulent lean premixed methane/air flame with $\phi = 0.60$. Also, what is the maximum flame temperature compared to the adiabatic flame temperature?

Author's Reply. For a laminar premixed methane/air flat flame with $\phi = 0.6$, the maximum measured temperature is approximately 20 K lower than the adiabatic flame temperature. Detailed chemistry calculations considering the radiation heat loss show that radiation from gaseous molecules is the direct and indirect cause of this temperature reduction.

●

Robert W. Pitz, Vanderbilt University, USA. Rather than modeling the turbulent temperature correlations, you could image a longer silicon carbide fiber and measure the instantaneous temperature distribution along the line of sight directly. Do you have any plans to measure these instantaneous temperature distributions and compare the measured correlations to your modeling results?

Author's Reply. We are in the process of making such measurements in our laboratory now.